

# I

## A new phase of matter?

### 1 Micro-bang and big-bang

#### 1.1 Energy and time scales

When atomic nuclei, generally called heavy-ions, collide at very high energies, such that the kinetic energy exceeds significantly the rest energy, dense hadronic\* matter is produced. We refer to these reactions as (ultra)relativistic heavy-ion, or nuclear, collisions. The energy density of hadronic matter with which we are concerned has a benchmark value of

$$\epsilon = 1 \text{ GeV fm}^{-3} = 1.8 \times 10^{15} \text{ g cm}^{-3}. \quad (1.1)$$

The corresponding relativistic matter pressure is

$$P \simeq \frac{1}{3}\epsilon = 0.52 \times 10^{30} \text{ bar}. \quad (1.2)$$

Dense matter with these properties must have existed in the early Universe about 10  $\mu\text{s}$  after the big-bang. It might have been recreated extremely rarely in interactions of very-high-energy cosmic-ray particles. Some astrophysical objects may reach these extreme conditions. It had been speculated that a catastrophic change in the Universe could ensue when these conditions are recreated in laboratory experiments, but these fears have been refuted [85].

Experimental study of the physics of the early Universe requires in principle a large, practically infinite, volume of matter. For this reason, it is necessary to study high-energy collisions of the heaviest nuclei, rather than the more elementary and simpler-to-handle interactions of protons or leptons. However, we cannot study in the laboratory physical systems

---

\* In Greek, *barys* means strong and heavy; *leptos* is weak, light; *mesos* is intermediate, and *hadros* is strong. Hadronic (strong) interactions involve baryons and mesons (heavy and semi-heavy particles) but not leptons, the light and relatively weakly interacting electrons, muons, the heavy tau, and nearly massless neutrinos.

larger in volume than lead (Pb) or gold (Au). Hence, it would seem that we will not be able to explore experimentally the properties of the phase transition involving the dissolution of hadronic particles, since it is known that genuine phase transitions cannot develop in finite physical systems. However, only for *non-relativistic finite systems* it is impossible to observe experimentally the discontinuous phase properties. In our case, the ability to produce particles from energy and the presence of virtual fluctuation effects greatly enhance the number of physical states accessible. We therefore hope to identify in collisions of relativistic heavy-ions a (nearly) singular manifestation of a phase transition from the nuclear, hadronic phase to a matter phase consisting of quarks and gluons.

We use units in which the Boltzmann constant  $k = 1$ . In consequence, the temperature  $T$  is discussed in units of energy, which, in this book, are either MeV  $\simeq 2m_e c^2$  ( $m_e$  is the electron mass) or GeV = 1000 MeV  $\simeq m_N c^2$  ( $m_N$  is the mass of a nucleon). The conversion scale of typical temperature involves ten additional zeros:

$$100 \text{ MeV} \equiv 116 \times 10^{10} \text{ K}. \quad (1.3)$$

To appreciate the magnitude of this temperature, let us recall that the center of the Sun is believed to be at  $T = 11 \times 10^6 \text{ K}$ , and the scale of temperature of interest to us is in fact 100 000 times greater.

In general, the units in this book are chosen such that the numerical values  $\hbar = c = 1$ , e.g., the mass of particles will also be measured in units of energy and the energy density can appear as the fourth power of an energy unit. With the conversion factor  $\hbar c = 0.197 \text{ GeV fm}$ , the reference energy density in normal nuclei is

$$\frac{m_N}{V_N} = 0.17 m_N \text{ fm}^{-3} \simeq 0.16 \text{ GeV fm}^{-3} = 1.27 \times 10^{-4} \text{ GeV}^4. \quad (1.4)$$

Experimental results have shown that ultra-relativistic heavy-ion collisions lead to the formation of a dense hadronic fireball, well localized in space, with an energy density exceeding  $1 \text{ GeV fm}^{-3}$ . Such a spatially localized drop of highly excited, hot, and dense *elementary matter* will be rapidly evolving, indeed exploding, driven by the high internal pressure. The fireball has a short life span characterized by the size of the system  $\tau \simeq 2R/c$ .

In relativistic heavy-ion reactions, the collision energy is shared among numerous newly produced hadronic particles. Therefore, in the final state we observe many soft (low-energy) newly produced hadronic particles, rather than a few particles of high-energy as is the case in hard, elementary interactions. An important objective of our research is the understanding of the processes that lead to the conversion of kinetic collision energy into high particle multiplicity. Because of the large numbers of

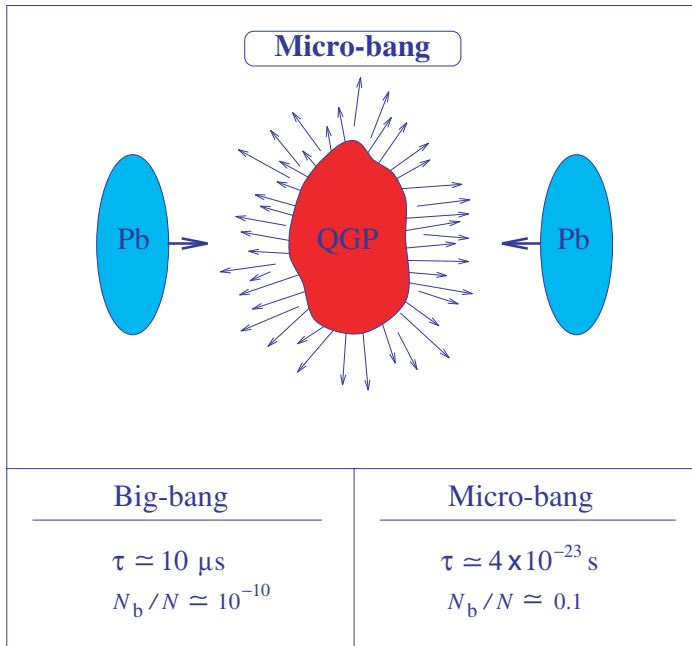


Fig. 1.1. Top: Lorentz-contracted nuclei collide in the center-of-momentum frame and form a region of dense matter, which evolves into a final state of hadrons. Bottom: two key differences involving baryon number  $N_b$  and total particle number  $N$  between the micro-bang and the cosmological big-bang.

particles produced, many thousands in recent experiments, we believe that this can be accomplished using statistical mechanics. This method has the advantage that it does not require a complete description of the microscopic production and dynamics of particles. It will be introduced in great detail in this book.

A qualitative image of the high-energy nuclear-collision ‘micro-bang’ is depicted in Fig. 1.1: two nuclei are shown, Lorentz-contracted in the direction of motion, approaching from two sides and colliding in the center-of-momentum (CM) laboratory frame, forming a region of dense matter (dark-shaded), the fireball. Subsequently, the collective expansion flow of fireball matter develops, and evolves in the final state into free streams of individual particles, indicated by individual arrows.

The temporal evolution of a fireball into a final state comprising a multitude of different hadronic particles is similar to, though much faster than, the corresponding stage in the evolution of the early Universe. Relativistic heavy-ion collision leads to a rapidly evolving fireball of quark–gluon plasma (QGP), in which the short time scale involved is probed by the equilibration of abundance of quark flavors. We can not hope to be able

to recreate the ‘slow big-bang’ of the Universe in the laboratory in the last detail. Our objective is to obtain precise information about the physical processes and parameters which govern the rapidly changing hadronic phase. Within a theoretical framework, we can hope to unravel what happened when the Universe hadronized.

The bottom portion of Fig. 1.1 reminds us of the two important differences between the two ‘bangs’, the big-bang of the Universe and the micro-bangs generated in the nuclear-collision experiments.

1. The time scale of the expansion of the Universe is determined by the interplay of the gravitational forces and the radiative and Fermi pressure of the hot matter, whereas in the micro-bangs there is no gravitation to slow the expansion, which lasts at most about  $10^{-22}$  s. The time scale of the heavy-ion collision, indicated in Fig. 1.1, suggests that the size and the (local) properties of the exploding nuclear fireball must change rapidly even on the scale of hadronic interactions, contrary to the situation in the early Universe. It is convenient to represent the expansion time constant  $\tau_U$  of the Universe in terms of the Newtonian gravitational constant  $G$  and the vacuum energy  $\mathcal{B}$ :

$$\tau_U = \sqrt{\frac{3c^2}{32\pi G\mathcal{B}}} = 36\sqrt{\frac{\mathcal{B}_0}{\mathcal{B}}} \mu\text{s}, \quad \mathcal{B}_0 = 0.19 \text{ GeV fm}^{-3} = (195 \text{ MeV})^4. \quad (1.5)$$

The range of values of the ‘bag’ constant  $\mathcal{B}$  found in the literature,  $145 \text{ MeV} < \mathcal{B}^{1/4} < 235 \text{ MeV}$ , leads to  $66 \mu\text{s} > \tau_U > 25 \mu\text{s}$ .

2. The early radiative Universe was practically baryonless, whereas in the laboratory we create a fireball of dense matter with a considerable baryon number  $N_b$  per total final particle multiplicity  $N$ . Thus, unlike in the early Universe, we expect in a laboratory micro-bang a significant matter–antimatter asymmetry in particle abundance. The matter–antimatter symmetry of particle spectra is in turn an important indicator suggesting that the matter–antimatter symmetry has been restored in other aspects.

The matter–antimatter-abundance asymmetry is easily overcome theoretically, since it implies a relatively minor extrapolation of the baryochemical potential  $\mu_b$  introduced to fix the baryon density. In fact, RHIC experiments at CM-energy  $130A$  GeV per pair of nucleons ( $\sqrt{s_{NN}} = 130$  GeV) are already much more baryon–antibaryon symmetric than the SPS condition where  $\sqrt{s_{NN}} \leq 17.3$  GeV, and the highest RHIC and LHC energies will allow us to extrapolate our understanding from  $\mu_b/T \leq 1$  to  $\mu_b/T \ll 1$ .

More difficult to resolve will be the differences in the physics due to the different time scales involved. The evolution of the Universe is slow on

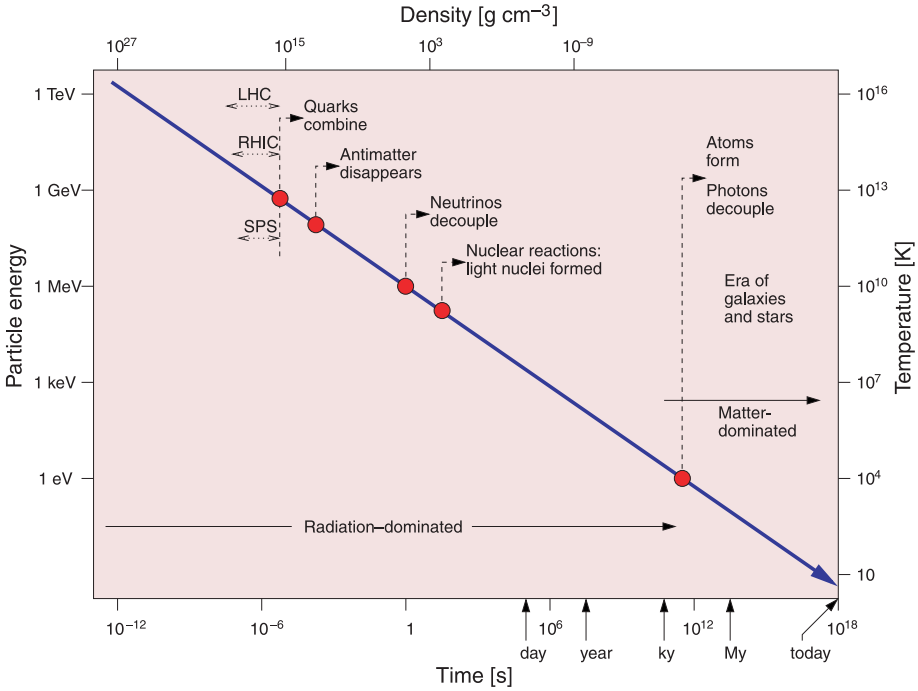


Fig. 1.2. Particle energy (temperature) as a function of time in the early Universe. Different evolutionary epochs are shown along with the accessible range of accelerator laboratory experiments.

the hadronic time scale. Given the value of  $\tau_U$ , we expect that practically all unstable hadronic particles decay, all hadronic equilibria are fully attained, and there is potentially time to develop macroscopic structures in the ‘mixed phase’ of QGP and hadronic gas (HG), and for weak interactions to take place. All this can not occur during the life span of the dense matter created in nuclear collisions.

The temporal evolution of the Universe is depicted, in Fig. 1.2, as a function of time. Beginning with decoupling of neutrinos and nucleosynthesis at time  $\mathcal{O}(1)$ s the evolution of the Universe is well understood today. In comparison, little work has gone into the detailed understanding of the earlier period when the nearly symmetric matter–antimatter hadron gas emerged from the quark–gluon phase and evolved into the baryon Universe in which we find ourselves today. This period spans the temperature interval  $300 \text{ MeV} < T < 1 \text{ MeV}$ , separating the perturbative QGP epoch from the epoch of decoupling of neutrinos and cosmological nucleosynthesis.

We see, in Fig. 1.2, that, after about  $10 \mu\text{s}$ , the deconfined phase of quarks and gluons is transformed into a hot gas of hadrons, namely mesons,

baryons, and antibaryons. Just after that, the evolution of our Universe was marked by a period of baryon–antibaryon annihilation, and, possibly, separation: although we have not been able to observe antimatter in our galaxy, or in the neighborhood of our galaxy, it is far from certain that there is no antimatter in our Universe.

The laboratory study of the formation of the QGP and hadronization is expected to lead to an understanding of how the hot, baryon- and antibaryon-rich hadron gas evolved after its formation at  $T \simeq 170$  MeV. Employing the statistical-physics methods developed in this book, one finds that the energy fraction of baryons and antibaryons within hadronic-gas matter is about 25% just after the QGP has hadronized in the early Universe, and nearly half of this is comprised of the heavier and unstable strange baryons and antibaryons. It is believed that this strong antimatter component disappears from the Universe prior to the era of nucleosynthesis.

## 1.2 Quarks and gluons

Both quarks and gluons manifest themselves only for a short instant following a high-energy interaction, and have never been observed as free objects at macroscopic distances from the space–time volume of the reaction; they are ‘confined’. Gluons interact only through strong interactions and pose a great experimental challenge regarding the study of their properties. The measurement of the properties of confined quarks is relatively easy, since, in addition to the strong-interaction (color) charge, they also carry the electro-weak charges.

There are six different *flavors* of quarks, see table 1.1, two practically stable flavors referred to as *up* – for the proton-like quark  $u$ , and *down* – for the neutron-like quark  $d$ . We often refer to these two light quarks by their generic name  $q$ . Light quarks  $q$  may be viewed as a single entity with two states, up or down. The semi-heavy *strange*-flavor  $s$ -quark decays due to electro-weak interaction when it is bound in hadrons, typically within  $10^{-10}$  s, whereas the heavier *charm*  $c$  and *bottom*  $b$  flavors have approximate life spans of  $3 \times 10^{-13}$  s and  $10^{-12}$  s, respectively.

These six flavors of quarks form three doublets:

$$\begin{pmatrix} u \\ d \end{pmatrix}, \quad \begin{pmatrix} c \\ s \end{pmatrix}, \quad \begin{pmatrix} t \\ b \end{pmatrix}; \quad Q_q = \begin{pmatrix} +\frac{2}{3} \\ -\frac{1}{3} \end{pmatrix}.$$

The upper component of a doublet has charge  $Q_q = +\frac{2}{3}$ , in units of the proton charge, whereas the lower component has one unit of charge less, as is also the case for the related lepton doublet comprising the three charged leptons (electron, muon, and tau) accompanied by their neutrinos. There is an antiquark for each quark, carrying the opposite electrical charge.

Table 1.1. Properties of quarks: flavor  $f$  symbol, flavor name, electrical charge  $Q_f$  (in units of proton charge  $Q_p$ ), and mass  $m_f$  at energy scale 2 GeV; see the text for further discussion of strange-quark mass

$f$	Quark	$Q_f [Q_p]$	$m_f(2 \text{ GeV})$
u	Up	$+\frac{2}{3}$	$3.5 \pm 2 \text{ MeV}$
d	Down	$-\frac{1}{3}$	$6 \pm 3 \text{ MeV}$
s	Strange	$-\frac{1}{3}$	$115 \pm 55 \text{ MeV}$
c	Charm	$+\frac{2}{3}$	$1.25 \pm 0.15 \text{ GeV}$
b	Bottom	$-\frac{1}{3}$	$4.25 \pm 0.15 \text{ GeV}$
t	Top	$+\frac{2}{3}$	$174.3 \pm 5.1 \text{ GeV}$

Quarks differ from charged leptons (electrons  $e$ , muons  $\mu$ , and taus  $\tau$ ), and neutrinos ( $\nu_i$ ,  $i = e, \mu$ , and  $\tau$ ) by a further internal quantum number they must carry, in addition to spin. The presence of this additional quantum number arises even in the simplest quark models. For example, consider hadronic particles containing three quarks of the same flavor, such as the spin-3/2 baryons:

$$\Delta^{++} = (uuu), \quad \Delta^- = (ddd), \quad \Omega^- = (sss).$$

The physical properties of these baryons imply that three identical quarks are present in the same S-wave with the same spin wave function. Since quarks are fermions, they are subject to the Pauli principle. Thus, there must be an additional way to distinguish the quarks, aside from spin. This additional degeneracy factor has been determined to be  $g_c = 3$ . It became known as the color of quarks – in analogy to the three fundamental colors: red, green, and blue.

Color is an internal quantum number, which like the electrical charge, is thought to be the source of a force [123]. It seems that there is no way to build an apparatus to distinguish the three fundamental color charges, all colors must everywhere be exactly equal physically. The theory of color forces must satisfy the principle of local nonabelian gauge invariance, e.g., invariance under arbitrary local  $SU(3)$  transformations in the three-dimensional color space. In other aspects, there is considerable formal similarity with quantum electrodynamics (QED). Therefore, the theory of strong interactions based on such color forces has been called quantum chromodynamics (QCD).

The flavor structure and symmetry of quarks and leptons remains a mystery today. We also do not have a fundamental understanding of the origin of quark masses. In table 1.1 we see that quarks of various flavors

differ widely in their ‘current’ mass  $m_f$ , that is mass which enters the elementary QCD Lagrangian  $\mathcal{L}_{\text{QCD}}$ . The values presented in table 1.1 are for the momentum scale 2 GeV.

Since quarks are confined inside hadrons, and the zero-point energy of confinement is much larger than the masses of light quarks, their masses could not be determined by direct measurement. However, the precise masses of light u and d quarks do not matter in the study of hadronic interactions, being generally much smaller than the pertinent energy scales,

The mass of the strange quark  $m_s$  is barely heavy enough to be determined directly in a study of hadronic structure. We adopt, in this book, the value  $m_s(1 \text{ GeV}) = 200 \pm 20 \text{ MeV}$  [150]. In the value of  $m_s$  reference is made to the scale of energy at which the mass of the strange quark is measured: akin to the interaction strength, also the mass of quarks depends on the (energy) scale. This value of  $m_s$  corresponds to  $m_s(2 \text{ GeV}) \simeq m_s(1 \text{ GeV})/1.30 = 154 \pm 15 \text{ MeV}$ . A somewhat smaller value  $m_s(2 \text{ GeV}) = 115 \pm 55 \text{ MeV}$ , see table 1.1, corresponding to  $m_s(1 \text{ GeV}) \simeq 150 \pm 70 \text{ MeV}$ , is the recommended value. The rather rapid change by 30% of the quark mass between the 1- and 2-GeV scales is well known, but often not remembered, e.g., the ‘low’ recommended mass of the charmed quark presented in table 1.1 in fact corresponds to  $m_c(1 \text{ GeV}) = 1.6 \text{ GeV}$ , a rather ‘high’ value.

### 1.3 The hadronic phase transition in the early Universe

We will now show that the ‘freezing’ of quark–gluon ‘color’ deconfined degrees of freedom is the essential ingredient in determining the conditions in a transition between phases that has time to develop into equilibrium. The following discussion tacitly assumes the presence of latent heat  $\mathcal{B}$  in the transition, and a discontinuity in the number of degrees of freedom,  $g_2 \neq g_1$ , where ‘1’ refers to the primeval QGP phase and ‘2’ to the final hadronic-gas state.

To find the phase-transition point, we determine the (critical) temperature at which the pressures in the two phases are equal. We allow, in a transition of first order, for a difference in energy density  $\epsilon_1 \neq \epsilon_2$  associated with the appearance of latent heat  $\mathcal{B}$  (the ‘bag constant’), which also enters the pressure of the deconfined phase. We consider the Stefan–Boltzmann pressure of a massless photon-like gas with degeneracy  $g_i$ :

$$P_c \equiv P_1(T_c) = \frac{\pi^2}{90} g_1 T_c^4 - \mathcal{B}, \quad (1.6)$$

$$P_c \equiv P_2(T_c) = \frac{\pi^2}{90} g_2 T_c^4. \quad (1.7)$$

We obtain

$$\frac{\mathcal{B}}{T_c^4} = \frac{\pi^2}{90} \Delta g, \quad T_c = \mathcal{B}^{\frac{1}{4}} \left( \frac{90}{\pi^2 \Delta g} \right)^{\frac{1}{4}}, \quad \Delta g = g_1 - g_2. \quad (1.8)$$

The transition temperature, in the early Universe, is slightly higher than the value seen in laboratory experiments, even though Eq. (1.8) involves only the difference in the number of degrees of freedom. For the pressure at the transition we obtain

$$P_c = \mathcal{B} \frac{g_2}{\Delta g}. \quad (1.9)$$

The pressure, and therefore the dynamics of the transition in the early Universe, depends on the presence of non-hadronic degrees of freedom, which are absent from laboratory experiments with heavy ions.

In summary, the phase-transition dynamics in the early Universe is determined by

- (a) the effective number of confined degrees of freedom,  $g_2$ , at  $T_c$ ;
- (b) the change in the number of acting degrees of freedom  $\Delta g$ , which occurs exclusively in the strong-interaction sector; and
- (c) the vacuum pressure (latent heat)  $\mathcal{B}$ , a property of strong interactions.

In order to understand the early Universe, we need to measure these quantities in laboratory experiments.

Both phases involved in the hadronization transition contain effectively massless electro-weak (EW) particles. Even though the critical temperature does not depend on the background of EW particles not participating in the transition, the value of the critical pressure, Eq. (1.9), depends on this, and thus we will briefly digress to consider the active electro-weak degrees of freedom. These involve photons,  $\gamma$ , and all light fermions, viz.,  $e$ ,  $\mu$ ,  $\nu_e$ ,  $\nu_\mu$ , and  $\nu_\tau$  (we exclude the heavy  $\tau$ -lepton with  $m_\tau \gg T$ , and we consider the muon as being effectively a massless particle). Near to  $T \simeq 200$  MeV, we obtain

$$g^{\text{EW}} = g_\gamma + \frac{7}{4} g_{\text{F}}^{\text{EW}} = 14.25, \quad (1.10)$$

with

$$g_\gamma = 2, \quad \frac{7}{4} g_{\text{F}}^{\text{EW}} = \frac{7}{8} \times 2 \times (2_e + 2_\mu + 3_\nu) = 12.25,$$

where charged, effectively massless fermions enter with spin multiplicity 2, and we have three neutrino flavors – there are only left-handed light neutrinos and right-handed antineutrinos, and thus only half as many neutrino degrees of freedom as would naively be expected.

In the deconfined QGP phase of the early Universe, we have

$$g_1 = g^{\text{EW}} + g_{\text{g}} + \frac{7}{4} g_{\text{q}}. \quad (1.11)$$

The number of effectively present strongly interacting degrees of freedom of quarks and gluons is influenced by their interactions, characterized by the strong coupling constant  $\alpha_s$ , and this book will address this topic in depth,

$$g_g = 2_s \times 8_c \left(1 - \frac{15}{4\pi} \alpha_s\right), \quad \frac{7}{4} g_q = \frac{7}{4} 2_s \times 2.5_f \times 3_c \left(1 - \frac{50}{21\pi} \alpha_s\right), \quad (1.12)$$

where the flavor degeneracy factor used is 2.5, allowing in a qualitative manner for the contribution of more massive strangeness; table 1.1. The degeneracies of quarks and gluons are indicated by the subscripts s(pin) and, c(olor), respectively. We obtain

$$g_1 = \begin{cases} 56.5, & \text{for } \alpha_s = 0, \\ \sim 37, & \text{for } \alpha_s = 0.5, \\ \sim 33, & \text{for } \alpha_s = 0.6. \end{cases} \quad (1.13)$$

For the QCD perturbative interactions with  $\alpha_s = 0.5\text{--}0.6$ , we see that  $g_1 \simeq 35 \pm 2$ .

We now consider the final HG phase of the early Universe: there is no light, strongly interacting fermion. Aside from three light bosons (pions  $\pi^\pm$  and  $\pi^0$ ), the presence of heavier hadrons contributes at  $T \lesssim 170$  MeV, and one finds for the hadronic degrees of freedom  $g_2^h \simeq 5$

$$g_2 \equiv g^{\text{EW}} + g_2^h \simeq 19. \quad (1.14)$$

Thus, we find from Eqs. (1.13) and (1.14),

$$g_1 - g_2 = \Delta g = \begin{cases} \sim 37, & \text{for } \alpha_s = 0, \\ \sim 18, & \text{for } \alpha_s = 0.5, \\ \sim 14, & \text{for } \alpha_s = 0.6. \end{cases} \quad (1.15)$$

For the QCD perturbative interactions with  $\alpha_s = 0.5\text{--}0.6$ , we see that about half of the degrees of freedom freeze across the transition in the early Universe.

For the value  $\mathcal{B}^{1/4} = 190$  MeV and  $\alpha_s \simeq 0.5$ , we obtain from Eq. (1.8) a transition temperature  $T_c \simeq 160$  MeV. At this temperature, the critical pressure Eq. (1.9) is found to be  $P_c \simeq 1.4 \mathcal{B}$ , and it includes both hadronic and electro-weak partial pressure contributions. The hadronic fractional pressure present in laboratory experiments and seen in lattice simulations of gauge theories (compare with section 15.5) is  $P_c^h \simeq \mathcal{B}/4$ .

#### 1.4 Entropy-conserving (isentropic) expansion

Much of the time dependence of an expanding Universe is related to the assumption of adiabatic, i.e., entropy-conserving, expansion dynamics:

$$dE + P dV = T dS = 0, \quad dE = d(\epsilon V), \quad \frac{dV}{V} = \frac{3 dR}{R}. \quad (1.16)$$